nature neuroscience

Functionally distinct inhibitory neurons at the first stage of visual cortical processing

Judith A Hirsch[1], Luis M Martinez[2], Cinthi Pillai[1], Jose-Manuel Alonso[3], Qingbo Wang[1] & Friedrich T Sommer[4]

Here we explore inhibitory circuits at the thalamocortical stage of processing in layer 4 of the cat's visual cortex, focusing on the anatomy and physiology of the interneurons themselves. Our immediate aim was to explore the inhibitory mechanisms that contribute to orientation selectivity, perhaps the most dramatic response property to emerge across the thalamocortical synapse. The broader goal was to understand how inhibitory circuits operate. Using whole-cell recording in cats *in vivo*, we found that layer 4 contains two populations of inhibitory cells defined by receptive field class—simple and complex. The simple cells were selective for stimulus orientation, whereas the complex cells were not. Our observations help to explain how neurons become sensitive to stimulus orientation and maintain that selectivity as stimulus contrast changes. Overall, the work suggests that different sources of inhibition, either selective for specific features or broadly tuned, interact to provide appropriate representations of elements within the environment.

There is little doubt that inhibition is centrally involved in visual cortical function, but there is much debate about what its precise role might be. Despite great interest and progress in the subject to date[1–4], our knowledge about inhibitory circuitry in visual cortex remains modest. Thus, we concentrated on exploring visual processing at the level of the interneurons themselves. Our focus was the earliest, or thalamocortical, stage of integration, where transformations in feature detection are famously pronounced[5]. Here, for the first time in the geniculostriate pathway, cells become able to resolve basic properties of a visual stimulus, such as orientation[5], and to preserve that selectivity as stimulus contrast changes[6,7]. In addition, studies of l ayer 4 are suited to comparison with those of inhibitory cells in somatosensory cortex, where response properties of interneurons are best understood[8–10]. The approach that we took was whole-cell recording *in vivo* with dye-filled electrodes combined with automated visual stimulation. The technique provided a way to characterize neural receptive fields and responses as well as to establish anatomical position and class[1,3,11–13]. Although interneurons are rare[12] and usually small[12], over time we were able to assemble a functional picture of inhibitory circuits that originate in cortical layer 4.

Before describing specific inhibitory contributions to cortical response pattern, it is important to provide a brief description of the physiology of layer 4. There, neurons divide into two main classes, simple and complex[5,14]; both types of cell receive direct thalamic input[15,16]. Simple cells, the majority[5,14], have receptive fields built of parallel, adjacent On and Off subregions in which stimuli of the opposite contrast evoke responses of the inverse sign, an arrangement known as push-pull[5,14,17–19]. Complex cells make up approximately a quarter of the layer[15,20]; these cells lack segregated subregions[5,14]. For complex cells in layer 4, stimuli of either polarity evoke excitation throughout the receptive field [15,20]—an arrangement known as push-push.

As the push-pull structure for the simple receptive field forms the basis for a prominent class of models of orientation selectivity[19], it is important to understand how that field is built. Many studies using cats suggest that the push, or excitation, originates from On and Off center relay cells whose receptive fields tile the On and Off subregions of the simple receptive fields[5,16–18,21,22]. The pull is commonly thought to stem from inhibitory simple cells whose subregions are shaped like those of their postsynaptic targets but have the opposite sign[17,19,22], though alternative models have been proposed[23–25]. We investigated whether such inhibitory simple cells exist and found that they do; as predicted, these cells had receptive fields and orientation tuning properties that mirror those of their excitatory counterparts.

With almost the same frequency as we recorded from interneurons with simple receptive fields, we recorded from ones with complex receptive fields. The complex interneurons differed from their simple neighbors both in receptive field structure and orientation selectivity. Specifically, the complex cells were largely insensitive to stimulus angle, much like their thalamic inputs. These complex cells are likely to play distinctive roles in processing, for example, providing a substrate for mechanisms of gain control[7,8,24–30].

In sum, our results revealed two functionally different types of interneuron in layer 4. One class had a simple receptive field and was orientation-selective. The other kind had a complex receptive field and

[1]Department of Biological Sciences, University of Southern California, 3641 Watt Way, Los Angeles, California 90089-2520, USA. [2]Department of Medicine, Campus de Oza, Universidad A Coruña, 15006 Spain. [3]Department of Biological Sciences, SUNY-Optometry, 33 West 42nd Street, New York, New York 10036, USA. [4]Redwood Neuroscience Institute, 1010 El Camino Real, Menlo Park, California 94025, USA. Correspondence should be addressed to J.A.H. (jhirsch@usc.edu).

Published online 16 November 2003; doi:10.1038/nn1152

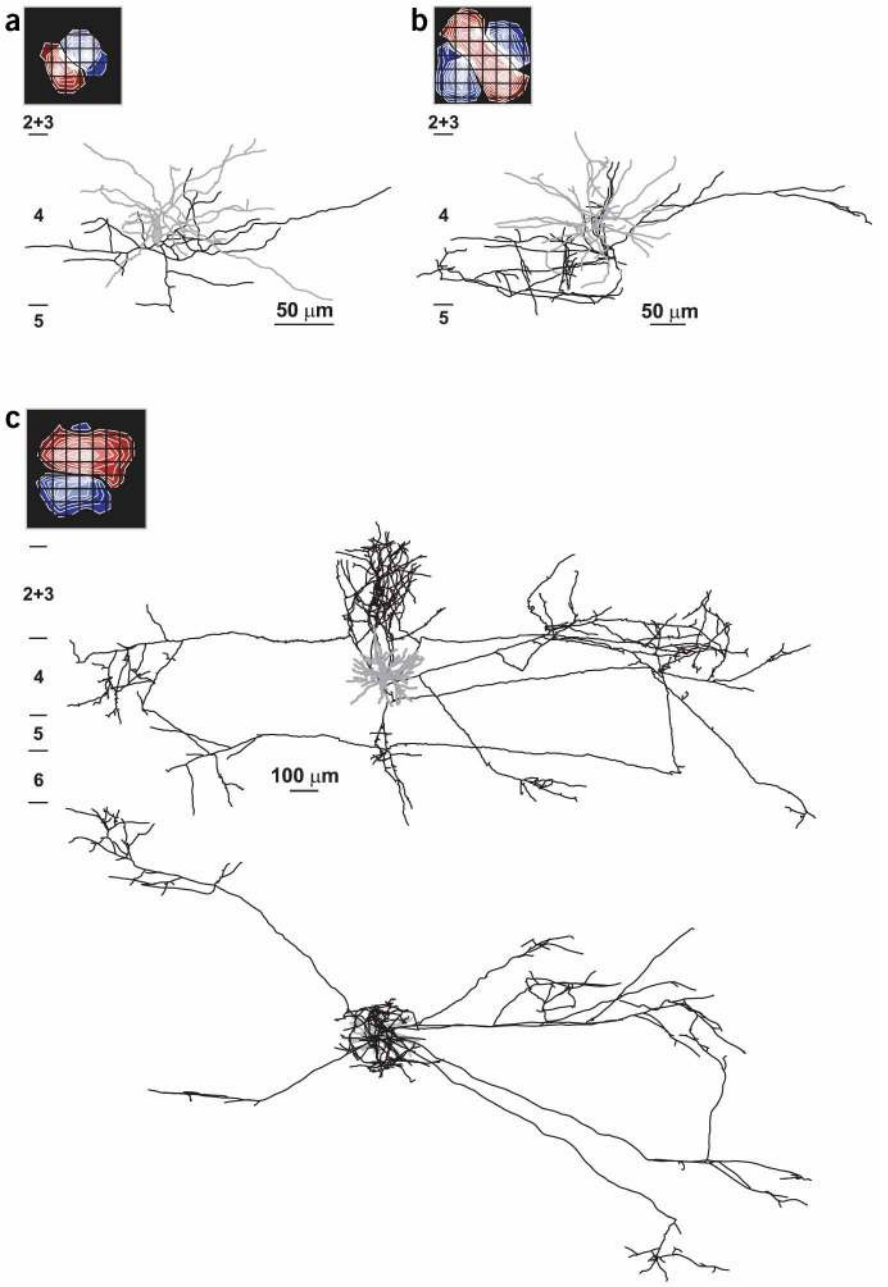

Figure 1 Morphology of smooth cells with simple receptive fields. (**a**) Coronal view of a flask-shaped neuron with beaded dendrites and partially labeled local axonal projections. In this and all figures, dendrites and cell bodies are shaded gray and axons black. (**b**) Coronal view of an interneuron with a radial dendritic arbor and an asymmetric projection pattern within layer 4. (**c**) Long range basket cell with a thick dendritic arbor in layer 4, dense projections to layer 2+3 and remote collaterals whose terminal clusters favor layers 4 and 6. For this cell the reconstruction is seen in both coronal (top) and tangential (bottom) views.

was not tuned for orientation. The concerted action of these cells not only helps to generate orientation sensitivity but also preserves that selectivity as stimulus strength changes[29,31]. More generally, our results raise the possibility that separate groups of interneurons, some selective for specific features of the stimulus and others not, help give rise to a feature-specific representation of the visual scene and the ability to maintain that picture over a wide range of contrasts[6,7,29,32].

RESULTS

Our results are from 11 adult cats. Of the ten smooth cells we examined in layer 4, six were simple and four were complex. A fifth complex cell recorded from upper layer 6, presumed inhibitory because of its membrane properties[33], had visual responses like those recorded from complex cells in layer 4.

Smooth simple cells

For many years, the circuit diagram for the push-pull model of the simple receptive field has been as follows: excitatory drive is supplied by convergent input from thalamic relay cells whose On or Off centers tile the On or Off subregions of simple cells (**Fig. 8a**, left). Inhibition is assumed to originate from interneurons whose receptive fields resemble those of their postsynaptic partners, save the component subregions have opposite preferences for stimulus contrast (**Fig. 8a**, middle). We now provide direct evidence that this inhibitory population exists.

Morphology

Drawings of three simple smooth cells accompanied by contour plots of their receptive fields are shown in **Fig. 1**. Although the cells were situated in mid layer 4 and had dendrites that largely respected laminar boundaries, each had a different axonal projection pattern. One neuron that had a flask-shaped soma (10 μm) and beaded dendrites[34–36] sent local projections within the home layer (**Fig. 1a**). Another cell had a smaller soma (7 μm) and smooth, radial dendrites; most of its axonal arbor swept to one side of the soma to course horizontally for 300 μm within the lower half of the layer, while sparser branches on the opposite side targeted the upper aspect of the lamina (**Fig. 1b**). A third interneuron, with a 14-μm soma, had an axon that ramified most densely in overlying layer 2 and 3 (layer 2+3). The cell also sent longer-range projections that terminated preferentially in layers 4 and 6 (**Fig. 1c**, top). The irregular spacing of these projections is seen in tangential view (**Fig. 1c**, bottom); collaterals traveling due right on the page emitted a web of branches in a region ~0.4–1.4 mm from the soma while the collaterals pointing bottom-right did not form clusters for lengths >1 mm. Thus, simple interneurons in layer 4 are a morphologically diverse group, with some providing local connections and others sending projections across the cortical depth and for long horizontal distances.

Receptive field structure

Is the variation known for receptive fields of excitatory simple cells matched by that seen in inhibitory simple cells? To make the comparison, we tapped our database of excitatory simple cells[22,37]. In each class of cell, spiny (**Fig. 2b**) and smooth (**Fig. 2a**), we found

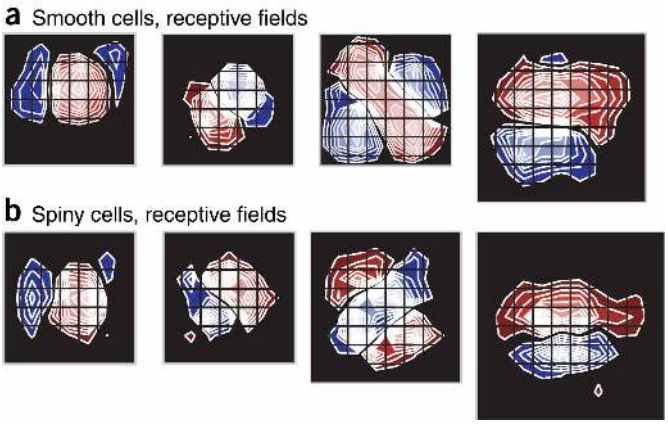

Figure 2 The receptive fields of smooth and spiny simple cells look alike. Contour plots of the receptive fields of four smooth (**a**) and four spiny (**b**) cells illustrate remarkable similarity between the two cell types. In this and all figures, On subregions are shown in red and Off subregions in blue. Within individual plots, each contour is smoothed and represents a 10% decrement from the peak value; brightness indicates the magnitude of response and the grid spacing was 0.85°. Action potentials were subtracted from the recordings before the maps were made.

cells with compact fields that have two or three subregions (**Fig. 2**, leftmost four panels) and with elongated fields with two or three subregions (**Fig. 2**, rightmost four panels). The range in length/width ratio for the strongest subregion of the receptive field for the smooth cells (1.2–3.4) was similar to that for spiny cells we had analyzed in a previous study[37] (1.3–4.0).

Similarity between the receptive field structure of the smooth and spiny[5,17,22,37,38] populations extended to the fine-grained level (**Fig. 3**); the push-pull pattern of excitation and inhibition was iterated point-by-point. In **Figure 3a**, the push-pull pattern is easy to see at the centers of each subregion (asterisks); for example, in the Off subregion, the introduction of a dark stimulus evoked a depolarization, and the withdrawal of the dark stimulus led to a hyperpolarization. Accordingly, a bright stimulus flashed at the same spot evoked inhibition followed by a prominent excitatory response that corresponded to the removal of the bright stimulus. This profile was seen throughout most of the field, with typical imbalances between the push and pull at some locations. A second example of the distribution of push and pull is shown in **Figure 3b** for the same cell drawn in **Figure 1c**. Although the cell was slightly hyperpolarized, thus reducing the amplitude of the inhibition compared to that of excitation, the overall pattern of spatially opponent excitation and inhibition was apparent. Furthermore, we measured the separation of subregions with an overlap index[39]; values ranged from ≤0 for separated subregions to 1 for superposition. For the population of simple cells, overlap indices ranged from –0.12 to 0.05, with an average of –0.06 ± 0.07 (mean ± s.d., $n = 5$).

Smooth simple cells also resembled spiny simple cells in the time course of response, which reprises and extends envelopes of thalamic activity[20,22]. For a representative population of spiny cells ($n = 10$), the latency was 23.8 ± 4 ms, and the duration of the excitatory responses to stimulus onset and withdrawal were 66.6 ± 18 ms and 165.9 ± 67.9 ms, respectively[20,22]. For five smooth cells, the corresponding values were similar ($P > 0.05$): 26.2 ± 4.0, 73.4 ± 8.0 and 129.4 ± 51.1 ms.

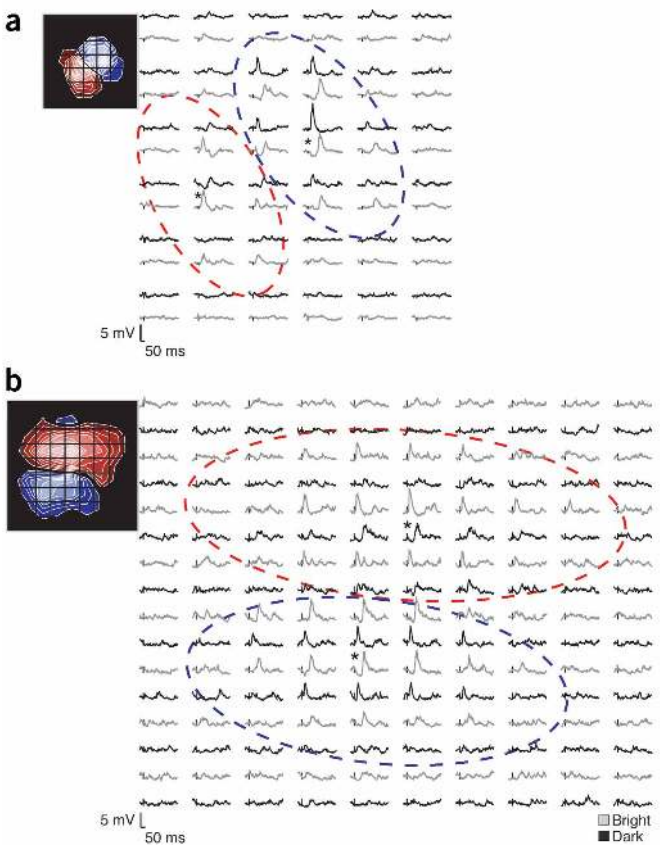

Figure 3 Push-pull structure of the smooth simple cell receptive field. (**a**) Receptive field of the simple cells drawn in **Fig. 1a**. (**b**) Receptive field of the simple cells drawn in **Fig. 1c**. Receptive fields are shown as an array of trace pairs in which each position in the grid is represented by the averaged responses to dark (black) and light (gray) squares flashed at the corresponding location. On and Off subregions are approximated by dotted ovals, and contour plots of the receptive fields are shown for reference. The small vertical dashes indicate the onset of the stimulus, which was flashed for 31 ms; stimulus size was 1.7° and the grid spacing was 0.85°. Asterisks denote a central point in each subregion.

Orientation tuning

Previous studies suggest that excitatory and inhibitory inputs to simple cells have the same preference for stimulus orientation[37,40]. To determine whether this arrangement is true for simple interneurons, we measured their orientation tuning by sweeping bars across their receptive fields (**Fig. 4**). A bright bar swept across the receptive field at the preferred orientation (**Fig. 4a**, top) produced a strong depolarization as it coursed through the On subregion, a hyperpolarization as it traveled through the Off subregion and then a strong excitatory response after leaving the Off subregion. This second depolarizing peak likely reflected the response of presynaptic Off-center relay cells to the departure of the bright stimulus from the center of their receptive fields. A bar tilted 45° from the preferred angle first passed over the upper-right portion of the On subregion and then simultaneously crossed portions of the On and Off subregions. Thus, the response began with a robust depolarizing component before adopting a low and irregular silhouette, presumably the result of mixed excitation and inhibition. Finally, the null-oriented stimulus, which fell over both subregions, evoked a weak, overall depolarizing response along its

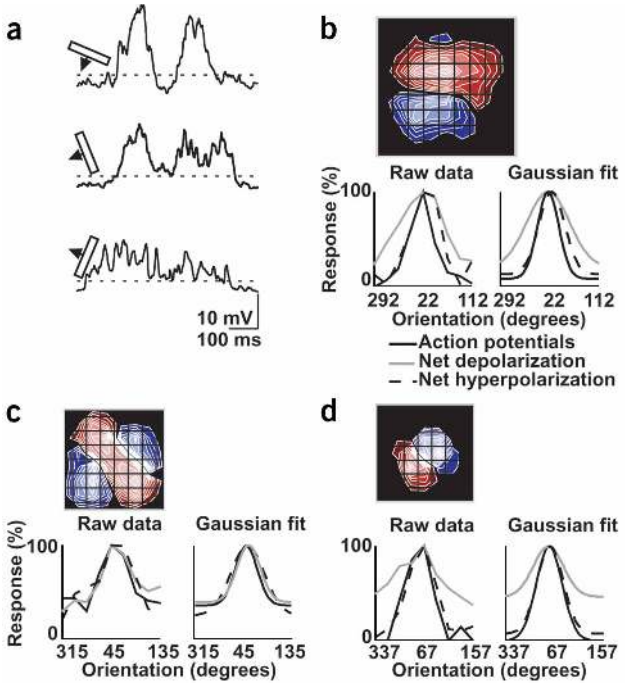

Figure 4 Smooth simple cells are orientation-selective. (**a**) These three traces illustrate the response of a simple cell (drawn in **Fig. 1c**) to presentation of bright bars at the preferred orientation (top), oblique (middle) and orthogonal (bottom) orientations; dashed lines indicate the resting level. (**b**) Contour plot of same cell's receptive field placed above (left) orientation tuning curves for depolarization (gray trace), hyperpolarization (dashed trace) and spikes (black trace) made from the neural responses to a full cycle of oriented stimuli. Right, the Gaussian fits of the data. (**c**,**d**) Contour plots and tuning curves for the same cells drawn in **Fig. 1a**,**c**.

course (**Fig. 4a**, bottom). Orientation tuning curves for the same cell were constructed from responses to bright and dark bars and are shown as plots made from the raw data and the Gaussian fits (**Fig. 4b**). Each graph includes three curves—for depolarization, or net excitation (gray line), hyperpolarization, or net inhibition (dashed line) and firing rate (black line); bandwidths were 48°, 31° and 24°, respectively, and all curves shared a common peak[37]. Results for two additional cells are plotted in **Figure 4c**,**d**: bandwidths were 48°, 51° and 36° and 62°, 31° and 24° respectively (further examples are provided in **Supplementary Fig. 1** online). For all six cells, the average bandwidths were 48.6 ± 15.8, 39.3 ± 20.6 and 26.6 ± 5.8. Unlike our earlier study[37], in which the average bandwidth for inhibition was 3° broader than that for excitation, here it was 9° narrower. This disparity likely reflects a difference in our protocols for smooth versus spiny cells. That is, for smooth cells, we often held the membrane potential well below spike threshold to reduce the risk of runaway activity that can obscure synaptic potentials and distort suprathreshold responses. By contrast, for most spiny cells, we were able to emphasize inhibition by recording at relatively depolarized voltages[37]. Still, the critical measure of bandwidth for excitation for the population of six smooth cells, 49 ± 17°, is not significantly different from 50°, the value we found for spiny cells[37]. Last, the average orientation indices, which measure depth of tuning, were 0.72 ± 0.14 for net excitation, 0.90 ± 0.12 for net inhibition, and 0.93 ± 0.12 for spikes.

Smooth complex cells: morphology

In addition to interneurons with simple receptive fields, layer 4 contains a group of smooth cells with complex receptive fields. Reconstructions of three such cells accompanied by plots of their receptive fields are shown in **Figure 5**. One interneuron had a small soma (12 μm) located at the upper border of layer 4. Its dendrites spread through upper layer 4 and lower layer 2+3, and its axon arborized densely within range of the dendrites (**Fig. 5a**). Most axon collaterals swept to one side of the soma, reaching 350 μm laterally, to innervate layer 2+3 and, more densely, layer 4. Sparser collaterals on the other side of the soma were more limited in lateral extent and preferred the upper portion of layer 4, though some reached layer 5. A second reconstruction (**Fig. 5b**) shows the dense axonal arbor of a basket cell in mid layer 4 (dendrites not recovered). The heavily branched axonal arbor spanned all layers of cortex, with the thickest projections carpeting a 450-μm swath of the full thickness of layer 4. Last, shown in two views, is a long-range basket cell whose soma (24 μm) was in mid layer 4 (**Fig. 5c**). The dendrites were largely restricted to the home layer, save one process that entered layer 2+3 and another that reached into layer 5. The vertically directed collaterals of the axonal arbor spanned the cortical depth, forming prominent clusters in the infragranular laminae (**Fig. 5c**, left). The horizontal extent of the arbor is best seen in tangential view (**Fig. 5c**, right).

Receptive field structure

The receptive field structure of the smooth complex cells in layer 4 was typical of complex excitatory cells in the layer; all responded to the sparse noise stimulus as if they received convergent input from overlapping populations of On and Off center relay cells[20]—push-push. This pattern is shown for two representative cells (**Fig. 6**). Stimuli of both polarities evoked similar responses, an initial and late depolarization often separated by a hyperpolarizing notch. As for all cells in layer 4, the depolarizations reflected the time course of thalamic responses to stimulus onset and withdrawal[20,22]. Responses to dark stimuli were more robust and widespread than those to light stimuli for the neuron in **Figure 6a** (same cell, **Fig. 5c**). In the second example, the responses to bright and dark stimuli were coextensive (**Fig. 6b;** same cell, **Fig. 5a**). All four of the cells had similar overlap indices, ranging 0.75–0.80, average 0.78 ± 0.03 ($n = 4$).

For the four smooth complex cells in layer 4, the average latency was 21 ± 2.2 ms, the duration of the initial depolarization was 54.5 ± 20.1 ms, and that of the late depolarization was 98.8 ± 32.6 ms (values for the cell in layer 6 were similar). The corresponding values for spiny complex or otherwise non-simple cells in layer 4 are not significantly different from those found in a recent study[20]: 25 ± 4, 67 ± 28 and 96 ± 28 ms ($n = 7$).

Orientation tuning

Unlike the simple cells, none of the smooth complex cells showed more than a weak bias for stimulus orientation (**Fig. 7a**). Responses to dark bars swept across the field (cell in **Fig. 5c**) are shown on the upper left. There was little systematic difference between the responses evoked by the most effective stimulus and those elicited by stimuli tilted 45° or 90° from that angle; each stimulus evoked an irregular, largely depolarizing waveform. This lack of orientation selectivity is captured by the orientation tuning curves and the fits of those curves (**Fig. 7b**). The range of response that we observed is illustrated in **Fig. 7c**,**d** (responses of the unlabeled cell in upper 6 were as in **Fig. 7d**). Further examples are provided in **Supplementary Fig. 1** online. Because responses to all orientations were robust (>75% of the peak response), we did not take measurements of bandwidth. The

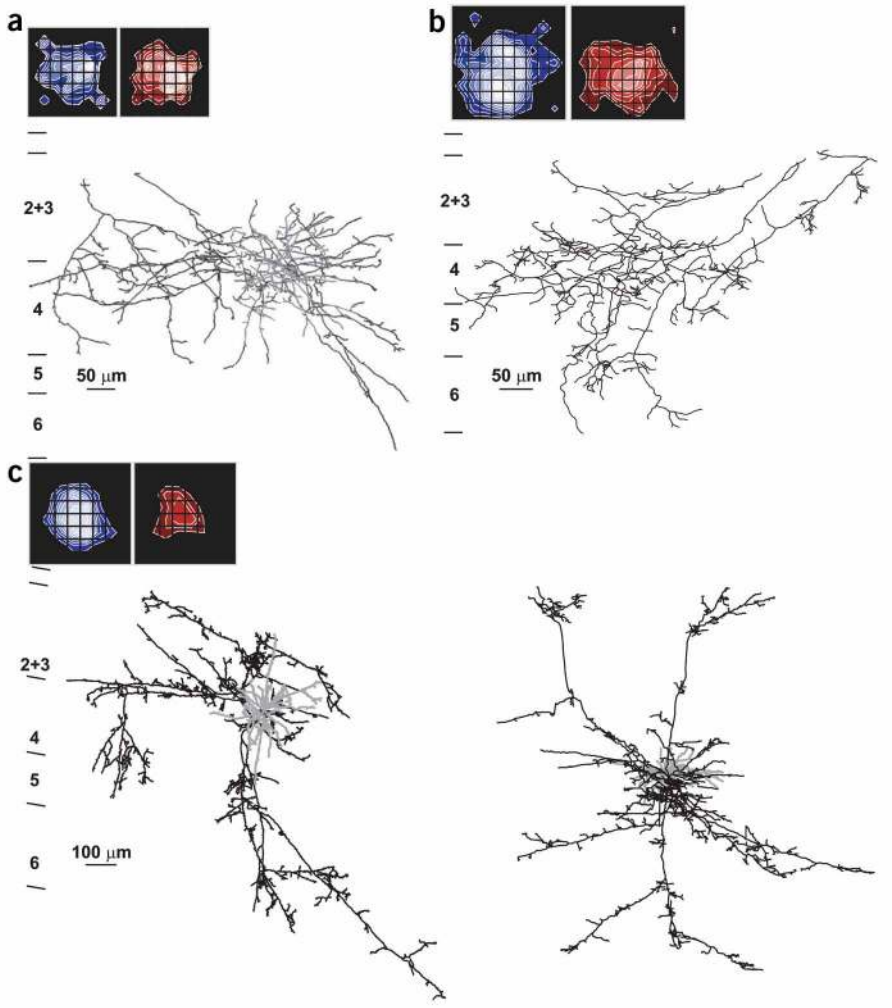

Figure 5 Morphology of smooth cells with complex receptive fields. (**a**) Coronal view of a basket cell at the border between layers 3 and 4, with especially dense projections in the upper half of layer 4. (**b**) Coronal view of the axon of a basket cell that projected densely throughout layer 4 as well as across the cortical depth. (**c**) Basket cell with dense local and vertical projections as well as longer-range collaterals that favored the border between layers 4 and 3 and loci in layer 5. Both a coronal (left) and tangential view (right) of the cell are shown. Accompanying contour plots of the receptive fields are shown as separate maps of bright and dark responses.

values of the orientation indices were small: 0.18 ± 0.04 for net excitation, 0.23 ± 0.08 for net inhibition and 0.31 ± 0.1 for spikes.

DISCUSSION

We explored the structure and function of the inhibitory circuits that contribute to visual processing in layer 4 of the cat's primary visual cortex by physiologically and anatomically characterizing interneurons. Our context was the emergence of orientation selectivity in layer 4, and our results are summarized in **Figure 8**. Feedforward models of orientation tuning (see ref. 19 for review) typically assume a push-pull circuit for the simple receptive field in which thalamic input initiates the push (**Fig. 8a**, left) and intracortical inhibition the pull (**Fig. 8a**, middle). Here we provided concrete evidence for the pull. Further, we showed that the simple interneurons have receptive field structures and orientation tuning properties indistinguishable from those of their spiny counterparts (**Fig. 8b**, left). Thus, it seems that all simple cells, both spiny and smooth, receive inhibitory input from simple cells. Moreover, our results revealed a second component of the inhibitory circuit in layer 4: a population of smooth cells with complex receptive fields that were neither sensitive to stimulus polarity nor orientation (**Fig. 8b**, right). This finding complements various models and previous experimental results that suggest that a source of untuned inhibition both sharpens sensitivity for certain stimulus features and maintains that sensitivity across contrasts[2,24,25,27–30]. A quantitative account of the differences between simple and complex interneurons is provided as a scatter plot (**Fig. 8c**) in which depth of tuning is plotted against degree of subregion overlap; simple and complex cells segregated along both axes. Last, each population of cell, simple and complex, sent projections that spanned all six layers of cortex as well as travel long (>1 mm) horizontal distances.

Receptive field structure

A first goal was to understand if the pull in the push-pull model of the simple receptive field could be reasonably explained by inhibitory simple cells. The receptive fields of simple cells vary in shape[5,14,17]. If the pull is to reflect the push, a straightforward way to achieve that balance would be a population of smooth cells with commensurately diverse receptive fields[19,41], which we found. The fine-grained structure of the receptive fields of the spiny and smooth cells was similar as well. Thus it seems that both spiny and smooth cells are built by similar mechanisms. Functionally, the receptive field structure of the simple interneurons cells provides a means to explain how intracortical inhibition may reduce activity driven by stimuli of uniform contrast that cross the border between subregions. This inhibition, for example, may have a role in improving orientation sensitivity, spatial frequency selectivity and specifying the spatial position of an object's border[5,17,29,31].

Four of the ten smooth cells we filled in layer 4 had complex receptive fields; the bulk of the projections they made were within the home layer. How would the input of these complex interneurons influence the spatial structure of receptive fields in layer 4? Imagine that a bright light fell within an On subregion of a simple cell that received input from simple and complex interneurons as pictured in **Fig. 8**. The thalamic excitation evoked by the bright stimulus might mask the inhibitory contribution of the complex interneuron[23–25,32,42], whereas the simple interneuron would be silent. If a dark stimulus were flashed in the same spot, inhibition from the simple and complex interneurons would sum as the pull. Thus the contribution of the smooth complex cells might not dictate the spatial structure of the receptive field *per se*, but rather modulate the overall level of inhibition[23–25,32,42].

Orientation tuning

The orientation tuning profiles of smooth simple cells were much like those described for simple cells in general—excitation and inhibition have similar preferences for stimulus angle[18,37,40] (compare to refs.

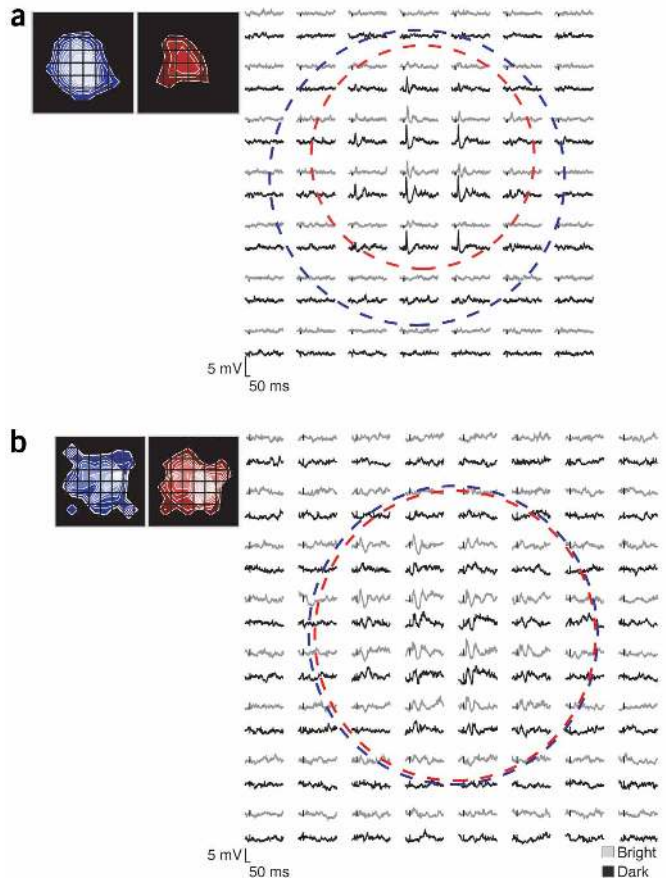

Figure 6 Push-push structure of the complex smooth cell receptive field. (**a**) Receptive field of the complex cell in **Fig. 5c** shown as an array of trace pairs with contour plots provided for reference; conventions as for **Fig. 3**. On responses fell within the regions of Off responses so that much of the receptive field was characterized by overlapping excitation to bright and dark stimuli. (**b**) Receptive field of the complex cell drawn in **Fig. 5a**. In this case, the On and Off subregions are nearly coextensive; stimulus size was 1.7° and the grid spacing was 0.85°.

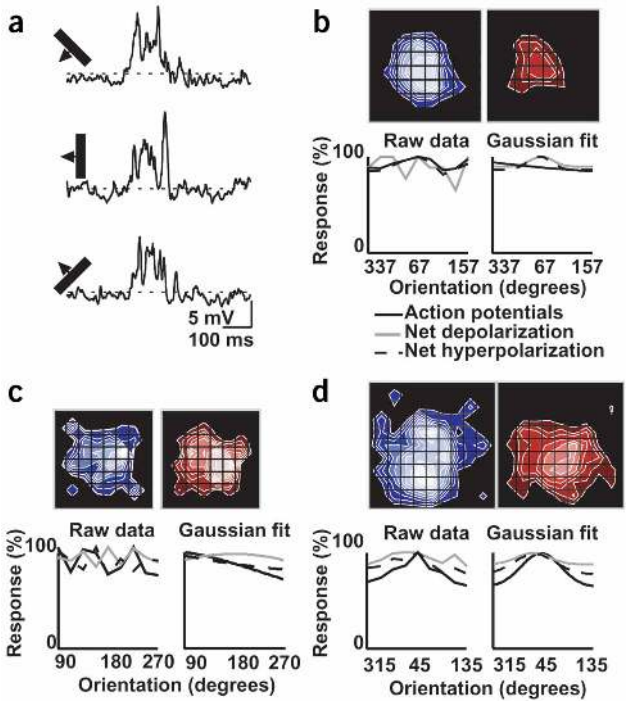

Figure 7 Smooth complex cells are not orientation-selective. (**a**) These three traces illustrate the response of a complex cell (in **Fig. 5c**) to dark bars at three orientations tilted 45° apart. (**b**) Contour plots of the receptive field atop orientation tuning curves for depolarization (gray trace), hyperpolarization (dashed trace) and spikes (black trace) made from the neural responses to a full cycle of oriented stimuli (left) and the Gaussian fits of those curves (right). The cell showed only a weak bias for orientation, as was typical for all other smooth complex cells; two additional examples are provided in panels **c** and **d**.

23,25,42). There is also a report of simple cells whose excitatory and inhibitory inputs do not share the same preference[25], but these cells may not have had simple receptive fields as originally defined[5]. Some term receptive fields with one subregion as simple[25,43] whereas we adopt a definition based on the presence of adjacent On and Off subregions[5]. In earlier studies, we found that receptive fields with only one subregion occupy later stages of processing[20] where the relative tuning of excitation and inhibition can diverge[37].

The orientation tuning of the complex smooth cells in layer 4 was like that of thalamic relay cells[7] rather than simple cells or complex cells at later cortical stages[37]. That is, the complex interneurons in layer 4 were excited nearly as strongly (>75%) by stimuli of any angle including the null[23,25,42]. Potential roles for this inhibition are discussed below. Finally, extracellular recordings in cat[15,43] and recent work in ferret[44] also show that layer 4 contains a population of untuned cells.

Push-pull and contrast-invariant orientation tuning

The push-pull model provides a framework for orientation tuning, but does a poor job of explaining how this selectivity is preserved as stimulus contrast rises[6,29,31]. In the thalamus, relay cells respond with increasing vigor to stimuli of all orientations as contrast grows. In the cortex, the picture is different. Although the peaks of cortical tuning curves grow taller as stimulus contrast rises, bandwidth does not broaden substantially[6,7]; that is, the level of cortical activity driven by orthogonal stimuli is not elevated by increased thalamic drive. What counters the contrast-dependent increase in 'untuned' thalamic firing to provide contrast-invariant orientation selectivity in cortex? If inhibitory simple cells resembled excitatory simple cells, they would be too weakly excited by null oriented stimuli to do the job[29,31]. Theoretical work[29,31] suggests that smooth simple cells might respond to all stimulus orientations and thus be able to cancel untuned thalamic drive; our results only partially support this idea. Although some smooth simple cells had broadly tuned responses to our full contrast stimuli and were substantially excited by orthogonal bars (see ref. 2), other cells were narrowly tuned and only moderately excited at the null.

The complex smooth cells in layer 4 add a new element to the local circuitry and essentially fill the gap that the past theoretical studies defined[29,31] and that recent theoretical work highlights[32]. That is, these cells produce a source of inhibition unselective for stimulus angle or polarity (phase). Given that the complex interneurons are strongly excited by stimuli of high contrast, they may well be able to contribute to contrast invariance and otherwise regulate levels of excitability.

Contrast invariance and orientation tuning in cat and primate

Prominent theories about orientation tuning in cats[25,27–29,42] and primates[24] rely on inhibition that is untuned or otherwise effective at the null orientation[26], which the smooth complex cells could provide[32].

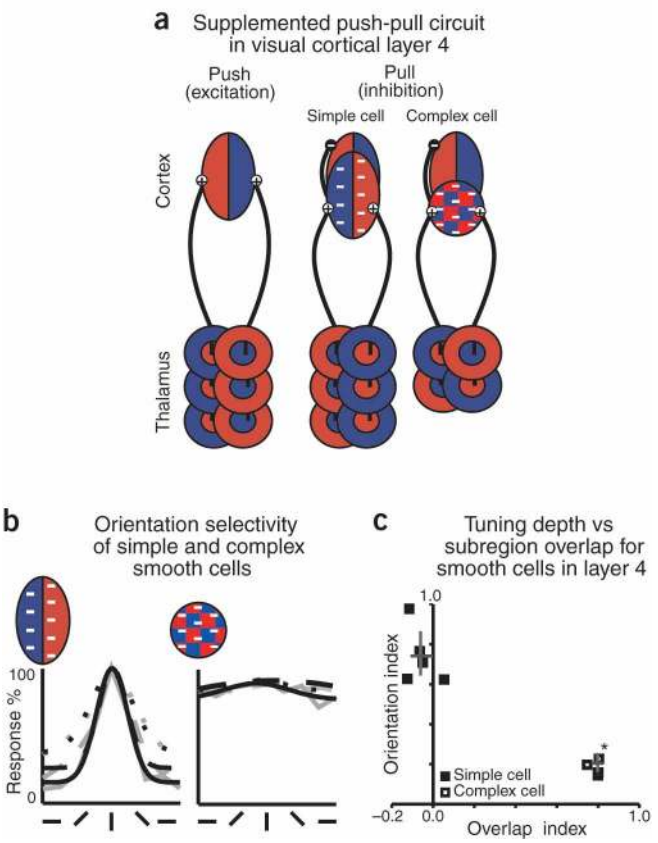

Figure 8 Summary of results. (**a**) Wiring diagrams of inputs to simple cells in layer 4. Cells are drawn as their receptive fields, minus signs label interneurons. Left, the push in simple subregions is built from adjacent, parallel rows of On and Off center thalamic relay cells. Middle, the pull is made by thalamic input routed through smooth simple cells whose receptive fields resemble those of their partners, except that overlapped subregions have the reverse polarity. Right, a second source of inhibition is provided by smooth complex cells that receive input from spatially overlapping On and Off center relay cells. Note that this scheme applies for the simple receptive fields of excitatory and inhibitory cells alike; that is, for each type of simple cell, thalamic input initiates the push while intracortical interneurons provide the pull. (**b**) Orientation selectivity of interneurons in layer 4. Averaged orientation tuning curves (gray) and their Gaussian fits (black) for simple cells ($n = 6$) and complex cells ($n = 4$), depolarization (dotted traces), hyperpolarization (dashed traces) and spikes (solid traces). (**c**) A comparison of receptive field structure and the depth of orientation tuning of interneurons of layer 4. Scatter plot comparing indices of subregion overlap with depth of orientation tuning. Results from simple cells are filled squares, open squares for complex cells, with the asterisk representing the putative smooth complex cell in layer 6. For the overlap index, values near 0 indicate separate subregions, and those near 1 indicate symmetrically overlapped subregions; for the orientation index, 0 indicates the absence of orientation selectivity and 1 the maximum depth of tuning. For each index, measurements were made from the net excitatory responses. The pair of gray crossed lines within each grouping of points (for simple and complex cells in layer 4) represents properties of the means of the orientation and overlap indices. The intersection of the lines corresponds to the mean values and the extension of the lines to the 95% confidence intervals (calculated with a bootstrap method).

Moreover, recent work suggests that both tuned and global sources of inhibition contribute to orientation dynamics in monkeys[30]. Although there are great differences in the laminar circuitry across species[11,13] and likely in the generation of orientation tuning[24,45], it is encouraging to imagine that our results illustrate principles that are evolutionarily conserved. Last, a recent model of suppressive mechanisms in cortex includes a role for synaptic depression[46], and our supplemented circuit for the push-pull model certainly does not exclude such a contribution.

Morphology of the inhibitory circuitry of layer 4

Our results complement existing profiles of inhibitory circuitry[1,3,4] by providing a detailed view of the functional characteristics of identified smooth cells. Each population of smooth cells, simple and complex, projected both within their home layers and columns and to remote sites. Unlike the horizontal connections sent by spiny cells[13,47], the longer-range projections of the smooth cells did not appear to cluster with regular periodicity, recalling a previous study[3] in which boutons of labeled basket cells were plotted over optically imaged maps of cortex to find diverse relationships between interneuronal output and functional architecture.

Comparison with somatosensory cortex

At the thalamocortical synapse in somatosensory cortex of rabbits and rodents, excitatory cells are sensitive to the direction of whisker displacement, whereas inhibitory (or suspected inhibitory[9,10]) cells are rarely so[8–10]. This disparity reflects a difference in thalamic input pattern; interneurons are supplied by multiple thalamic fibers each tuned to a different direction of motion, whereas excitatory cells are likely to receive a narrower projection[8,9]. The massive convergence of feedforward input to interneurons leads to fast, sensitive, synchronized responses that damp delayed or weak excitation[8–10,48].

How does inhibitory circuitry in the cat's visual cortex compare to that in the rabbit's somatosensory cortex? The chief similarity between the two areas is the presence of interneurons untuned for stimulus feature. Only the visual cortex, however, includes a prominent group of feature-specific smooth cells. In addition, the way that receptive fields for spiny and smooth cells are made may differ according to cortical area. Receptive fields of excitatory and inhibitory cells in the somatosensory cortex are probably constructed by separate patterns of thalamic input that, for the latter, are specialized for timing[9,10,49] . Although cells in layer 4 of the visual cortex also fall into different groups based on receptive field type—simple or complex, each apparently built by a different arrangement of thalamic input—there is not a parallel divide between excitatory and inhibitory cells. That is, in layer 4, spiny and smooth simple cells have similar receptive fields, as do spiny and smooth complex cells[20]. Hence, strategies for processing different types of sensory information may be related but not necessarily the same.

METHODS

Physiological preparation. Experimental subjects were adult cats (1.5–3.5 kg). We used standard methods for anesthesia, surgery and refracting the eyes as described in earlier studies[20,37]. All procedures were approved by the Institutional Animal Care and Use Committees of Rockefeller University and USC in accordance with the guidelines of the National Institutes of Health.

Recording and data acquisition and membrane properties. The methods used for recording were identical to those used in earlier studies[20,37]. Voltage-current relationships were measured before and after each stimulus cycle to monitor changes in the access and input resistances, threshold for firing and membrane time constant (range 6–28 ms). It was often impractical to assign absolute resting potential, as the ratio of access to seal resistance led to a voltage division of the neural signal[22]. Moreover, we could not always resolve entire spikes because fast events were filtered by the recording circuit, though shapes of undershoots

were preserved so that we were able to characterize smooth cells as fast ($n = 10$) or low threshold spiking ($n = 1$, see **Fig. 1a**)[33–36].

Receptive-field mapping. Receptive fields were hand-plotted to position the stimulus monitor and then mapped quantitatively with a modified[22] sparse noise protocol[17]; individual light and dark squares were flashed briefly (31–38 ms) in pseudo-random order 16 times on a 16 × 16 square grid; square size, 0.85–1.7°; contrast, 50–70%. Receptive fields were classified as simple or complex based on response to the sparse noise[5,14,17,20,22], except for one simple cell classified from responses to moving bars. Cells were classified as simple if their receptive fields included adjacent On and Off subregions: bright stimuli excite and dark ones inhibit in On subregions, and the reverse is true in Off subregions (push-pull)[43]. Complex cells were defined by their lack of segregated On and Off subregions. The complex cells in layer 4 had spatially overlapping excitatory responses to bright and dark stimuli (push-push). By contrast, some complex cells in regions not contacted by thalamic afferents (*e.g.*, layers 2+3 or 5) respond to only one polarity of the stimulus (push-null). Although we did not test cells with sinusoidal gratings, it is likely that the simple cell's responses would have tracked the fundamental frequency, as might have some complex cells more responsive to stimuli of one polarity than the other[50].

Plots of receptive fields were made in two ways, as contour plots or as arrays of trace pairs. For simple receptive fields, contour plots were made by subtracting dark from bright (spike subtracted) responses, whereas for complex receptive fields, plots for bright and dark stimuli are shown separately. For the arrays of trace pairs, each position on the stimulus grid is represented by two stacked traces showing the (spike subtracted) average to all bright or dark stimuli flashed at that point.

Last, we described the spatial structure of receptive fields by means of an overlap index[39]:

$$\text{Overlap index} = \frac{0.5W_p + 0.5W_n - d}{0.5W_p + 0.5W_n + d}$$

where W_p and W_n are the widths of the On and Off subregions, respectively, and d is the distance between the peak positions of the response to dark and bright stimuli. The value of the index is negative for separated subregions and approaches 1 for subregions that overlap symmetrically.

The parameters used to calculate the index were obtained by fitting each subregion (the excitatory responses to bright or to dark stimuli) with an elliptical Gaussian:

$$f(x, y) = \frac{A}{2\pi ab} \exp\left(-\frac{x'^2}{2a^2} - \frac{y'^2}{2b^2}\right)$$

for which A is the amplitude of the Gaussian, a and b are the half axes of the ellipse, and the quantities x' and y' are transformations of the coordinates x and y, taking into account the angle of the ellipse and its offset (x_c and y_c) with respect to the stimulus grid. Thus, there were six free parameters in the fitting procedure. To minimize the mean square error between the data and the fitting function, we used the Nelder-Mead simplex direct search (fminsearch in Matlab, MathWorks). The width of each subregion width was measured at 5% of the maximal height of the Gaussian, and the position of the peak was taken from the maximum of the Gaussian. For cells with three subregions, we used the average of the indices describing the offset between the center and each flank.

Measuring orientation tuning. Orientation tuning curves were made from responses to 4–8 repetitions of a bar swept at the best direction for eight different orientations for 180° of visual space; bar width, 0.85°; velocity, 10°/s; angular resolution, 22°; contrast, 100%. Net excitation (depolarization) was defined as the part of the response that fell between rest and more positive voltages; net inhibition (hyperpolarization) was defined in a similar way (measures were made from spike-subtracted records). For simple cells, measurements were confined to a time window set by the duration of the strongest depolarizing response evoked from the strongest subregion by optimally oriented bars (bright and dark); the window was centered on the peak response at each orientation. This normalization procedure corrected for differences in the time taken for stimuli to cross the length versus width of elongated subregions[37]. As complex receptive fields were not elongated, it was not necessary to use a window[37]. Each tuning curve was fit to a Gaussian function:

$$f(x) = \frac{A}{w\sqrt{2\pi}} \exp\left(-\frac{(x - x_c)^2}{2w^2}\right) + y_o$$

where y_0 = offset; x_c = center; w =standard deviation and A = area. Orientation preference was defined as the center of the Gaussian (x_c) and bandwidth as half-width at half-height.

Since some cells have flat tuning curves, they are not well described by Gaussians[2]. Thus, we provide an alternate description of orientation selectivity that measures the depth of tuning[2]:

$$\text{Orientation index} = \frac{R_{max} - R_{min}}{R_{max}}$$

where R_{max} is the maximum response and R_{min} the minimal response to the moving bars described above.

Morphological identification. After perfusion and histological processing[22], labeled neurons were drawn using a camera lucida or a computerized system (Microbrightfield, Inc.). Inhibitory cells were identified by anatomical convention; they typically have sparsely spinous or aspinous (smooth) dendrites and axonal arbors that differ from those of excitatory cells[1,3,4,11,12,33].

Note: Supplementary information is available on the Nature Neuroscience website.

ACKNOWLEDGMENTS

We thank T.N. Wiesel for discussions, K.D. Miller for improving the manuscript, R.C. Reid for contributing software and C.G. Marshall, K.D. Naik and J.M. Provost for assistance with the reconstructions. Supported by National Institutes of Health EY09593 to J.A.H.

COMPETING INTERESTS STATEMENT

The authors declare that they have no competing financial interests.

Received 30 August; accepted 16 October 2003
Published online at http://www.nature.com/natureneuroscience/

1. Martin, K.A., Somogyi, P. & Whitteridge, D. Physiological and morphological properties of identified basket cells in the cat's visual cortex. *Exp. Brain Res.* **50**, 193–200 (1983).
2. Azouz, R., Gray, C.M., Nowak, L.G. & McCormick, D.A. Physiological properties of inhibitory interneurons in cat striate cortex. *Cereb. Cortex* **7**, 534–545 (1997).
3. Buzas, P., Eysel, U.T., Adorjan, P. & Kisvarday, Z.F. Axonal topography of cortical basket cells in relation to orientation, direction, and ocular dominance maps. *J. Comp. Neurol.* **437**, 259–285 (2001).
4. Thomson, A.M. & West, D.C. Presynaptic frequency filtering in the gamma frequency band; dual intracellular recordings in slices of adult rat and cat neocortex. *Cereb. Cortex* **13**, 136–143 (2003).
5. Hubel, D.H. & Wiesel, T.N. Receptive fields, binocular interaction and functional architecture in the cat's visual cortex. *J. Physiol. (Lond.)* **160**, 106–154 (1962).
6. Sclar, G. & Freeman, R.D. Orientation selectivity in the cat's striate cortex is invariant with stimulus contrast. *Exp. Brain Res.* **46**, 457–461 (1982).
7. Ohzawa, I., Sclar, G. & Freeman, R.D. Contrast gain control in the cat's visual system. *J. Neurophysiol.* **54**, 651–667 (1985).
8. Bruno, R.M. & Simons, D.J. Feedforward mechanisms of excitatory and inhibitory cortical receptive fields. *J. Neurosci.* **22**, 10966–10975 (2002).
9. Swadlow, H.A. & Gusev, A.G. Receptive-field construction in cortical inhibitory interneurons. *Nat. Neurosci.* **5**, 403–404 (2002).
10. Swadlow, H.A. Fast-spike interneurons and feedforward inhibition in awake sensory neocortex. *Cereb. Cortex* **13**, 25–32 (2003).
11. Lund, J.S., Henry, G.H., MacQueen, C.L. & Harvey, A.R. Anatomical organization of the primary visual cortex (area 17) of the cat. A comparison with area 17 of the macaque monkey. *J. Comp. Neurol.* **184**, 599–618 (1979).
12. Gabbott, P.L. & Somogyi, P. Quantitative distribution of GABA-immunoreactive neurons in the visual cortex (area 17) of the cat. *Exp. Brain Res.* **61**, 323–331 (1986).
13. Callaway, E.M. Local circuits in primary visual cortex of the macaque monkey. *Annu. Rev. Neurosci.* **21**, 47–74 (1998).

14. Gilbert, C.D. Laminar differences in receptive field properties of cells in cat primary visual cortex. *J. Physiol. (Lond.)* **268**, 391–421 (1977).
15. Bullier, J. & Henry, G.H. Ordinal position of neurons in cat striate cortex. *J. Neurophysiol.* **42**, 1251–1263 (1979).
16. Tanaka, K. Organization of geniculate inputs to visual cortical cells in the cat. *Vision Res.* **25**, 357–364 (1985).
17. Jones, J.P. & Palmer, L.A. The two-dimensional spatial structure of simple receptive fields in cat striate cortex. *J. Neurophysiol.* **58**, 1187–1211 (1987).
18. Ferster, D. Orientation selectivity of synaptic potentials in neurons of cat primary visual cortex. *J. Neurosci.* **6**, 1284–1301 (1986).
19. Ferster, D. & Miller, K.D. Neural mechanisms of orientation selectivity in the visual cortex. *Annu. Rev. Neurosci.* **23**, 441–471 (2000).
20. Hirsch, J.A. *et al.* Synaptic physiology of the flow of information in the cat's visual cortex *in vivo*. *J. Physiol. (Lond.)* **540**, 335–350 (2002).
21. Reid, R.C. & Alonso, J.M. Specificity of monosynaptic connections from thalamus to visual cortex. *Nature* **378**, 281–284 (1995).
22. Hirsch, J.A., Alonso, J.M., Reid, R.C. & Martinez, L.M. Synaptic integration in striate cortical simple cells. *J. Neurosci.* **18**, 9517–9528 (1998).
23. Borg-Graham, L.J., Monier, C. & Fregnac, Y. Visual input evokes transient and strong shunting inhibition in visual cortical neurons. *Nature* **393**, 369–373 (1998).
24. Wielaard, D.J., Shelley, M., McLaughlin, D. & Shapley, R. How simple cells are made in a nonlinear network model of the visual cortex. *J. Neurosci.* **21**, 5203–5211 (2001).
25. Monier, C., Chavane, F., Baudot, P., Borg-Graham, L.J. & Fregnac, Y. Orientation and direction selectivity of synaptic inputs in visual cortical neurons: a diversity of combinations produces spike tuning. *Neuron* **37**, 663–680 (2003).
26. Burr, D., Morrone, C. & Maffei, L. Intra-cortical inhibition prevents simple cells from responding to textured visual patterns. *Exp. Brain Res.* **43**, 455–458 (1981).
27. Sillito, A.M. GABA mediated inhibitory processes in the function of the geniculostriate system. *Prog. Brain Res.* **90**, 349–384 (1992).
28. Somers, D.C., Nelson, S.B. & Sur, M. An emergent model of orientation selectivity in cat visual cortical simple cells. *J. Neurosci.* **15**, 5448–5465 (1995).
29. Troyer, T.W., Krukowski, A.E., Priebe, N.J. & Miller, K.D. Contrast-invariant orientation tuning in cat visual cortex: thalamocortical input tuning and correlation-based intracortical connectivity. *J. Neurosci.* **18**, 5908–5927 (1998).
30. Ringach, D.L., Hawken, M.J. & Shapley, R. Dynamics of orientation tuning in macaque V1: the role of global and tuned supression. *J. Neurophysiol.* **90**, 342–352 (2003).
31. Troyer, T.W., Krukowski, A.E. & Miller, K.D. LGN input to simple cells and contrast-invariant orientation tuning: an analysis. *J. Neurophysiol.* **87**, 2741–2752 (2002).
32. Lauritzen, T.Z. & Miller, K.D. Different roles for simple- and complex-cell inhibition in V1. *J. Neurosci.* (in press).
33. Nowak, L.G., Azouz, R., Sanchez-Vives, M.V., Gray, C.M. & McCormick, D.A. Electrophysiological classes of cat primary visual cortical neurons *in vivo* as revealed by quantitative analyses. *J. Neurophysiol.* **89**, 1541–1566 (2003).
34. Hirsch, J.A. Synaptic integration in layer IV of the ferret striate cortex. *J. Physiol. (Lond.)* **483**, 183–199 (1995).
35. Gibson, J.R., Beierlein, M. & Connors, B.W. Two networks of electrically coupled inhibitory neurons in neocortex. *Nature* **402**, 75–79 (1999).
36. Porter, J.T., Johnson, C.K. & Agmon, A. Diverse types of interneurons generate thalamus-evoked feedforward inhibition in the mouse barrel cortex. *J. Neurosci.* **21**, 2699–2710 (2001).
37. Martinez, L.M., Alonso, J.M., Reid, R.C. & Hirsch, J.A. Laminar processing of stimulus orientation in cat visual cortex. *J. Physiol. (Lond.)* 321–333 (2002).
38. Hirsch, J.A. Synaptic physiology and receptive field structure in the early visual pathway of the cat. *Cereb. Cortex* **13**, 63–69 (2003).
39. Schiller, P.H., Finlay, B.L. & Volman, S.F. Quantitative studies of single-cell properties in monkey striate cortex. I. Spatiotemporal organization of receptive fields. *J. Neurophysiol.* **39**, 1288–1319 (1976).
40. Anderson, J., Carandini, M. & Ferster, D. Orientation tuning of input conductance, excitation, and inhibition in cat primary visual cortex. *J. Neurophysiol.* **84**, 909–926 (2000).
41. Kayser, A.S. & Miller, K.D. Opponent inhibition: a developmental model of layer 4 of the neocortical circuit. *Neuron* **33**, 131–142 (2002).
42. Volgushev, M., Pei, X., Vidyasagar, T.R. & Creutzfeldt, O.D. Excitation and inhibition in orientation selectivity of cat visual cortex neurons revealed by whole-cell recordings *in vivo*. *Vis. Neurosci.* **10**, 1151–1155 (1993).
43. Henry, G.H. Receptive field classes of cells in the striate cortex of the cat. *Brain Res.* **133**, 1–28 (1977).
44. Usrey, W.M., Sceniak, M.P. & Chapman, B. Receptive fields and response properties of neurons in layer 4 of ferret visual cortex. *J. Neurophysiol.* **89**, 1003–1015 (2003).
45. Chisum, H.J., Mooser, F. & Fitzpatrick, D. Emergent properties of layer 2/3 neurons reflect the collinear arrangement of horizontal connections in tree shrew visual cortex. *J. Neurosci.* **23**, 2947-2960 (2003).
46. Carandini, M., Heeger, D.J. & Senn, W. A synaptic explanation of suppression in visual cortex. *J. Neurosci.* **22**, 10053–10065 (2002).
47. Gilbert, C.D. & Wiesel, T.N. Morphology and intracortical projections of functionally characterised neurones in the cat visual cortex. *Nature* **280**, 120–125 (1979).
48. Moore, C.I., Nelson, S.B. & Sur, M. Dynamics of neuronal processing in rat somatosensory cortex. *Trends Neurosci.* **22**, 513–520 (1999).
49. Brecht, M. & Sakmann, B. Dynamic representation of whisker deflection by synaptic potentials in spiny stellate and pyramidal cells in the barrels and septa of layer 4 rat somatosensory cortex. *J. Physiol. (Lond.)* **543**, 49–70 (2002).
50. Skottun, B.C. *et al.* Classifying simple and complex cells on the basis of response modulation. *Vision Res.* **31**, 1079–1086 (1991).